

# Atomic and nuclear $\Xi^-$ bound states

Author: Antoni Valls Cifre

Facultat de Física, Universitat de Barcelona, Diagonal 645, 08028 Barcelona, Spain.

Advisor: Àngels Ramos

**Abstract:** An study of the  $\Xi^-$ -nucleus interaction is done for the purpose of expanding the knowledge on how strangeness  $S = -2$  hyperons interact with nuclear media. Our work is based on some recent two-body capture events ( $\Xi^- p \rightarrow \Lambda\Lambda$ ) on  $^{12}\text{C}$  and  $^{14}\text{N}$  nuclei measured at KEK and J-PARC in which a pair of single- $\Lambda$  hypernuclei are formed. By developing an algorithm, based on Numerov's method, able to resolve numerically the radial Schrödinger's equation with a potential composed by a finite-size Coulomb potential and a nuclear potential shaped as a Woods-Saxon function, we conclude that this capture events occur from  $1p_{\Xi^-}$  nuclear states with a corresponding potential depth of  $V_0 \sim 14 - 17$  MeV. Developing a program able to find the  $\Xi^-$ -nuclear energy levels and their dependence on  $V_0$ , which is at the same time easy to adapt to other interacting particles or nuclei, is part of our intention here too.

## I. INTRODUCTION

The  $\Xi$  baryons, historically called *cascade particles* because of their tendency in decaying rapidly into lighter particles, are a family of baryons which consist of one up or down quark and two other, more massive quarks: strange, charm or bottom. The main cascade baryon for our study is  $\Xi^-$ , which is made of one down and two strange quarks (dss). Interest in the nuclear interaction of  $\Xi^-$  hyperons has been recently increased, as result of the latest  $\Xi^- p$  correlation studies measured by ALICE [1–4] in  $pp$  and  $p$ -Pb ultra-relativistic collisions.

Some work has already been done aiming to understand nuclear strong interaction in the strangeness  $S = -2$  sector. Old emulsion experiments, where the  $\Xi^-$  is captured in the emulsion and the decay products are observed, suggested an attractive  $\Xi^-$ -nuclear potential of  $V_{\Xi} \sim 21 - 24$  MeV [5]. However, dedicated ( $K^-, K^+$ ) counter experiments, driven by  $K^- p \rightarrow K^+ \Xi^-$  strangeness exchange on protons, where the produced  $\Xi^-$  hyperons populate predominantly the quasi-free continuum region, with less than 1% of events corresponding to  $\Xi^-$ -nuclear bound states, give shallower potentials of around  $V_{\Xi} \sim 15$  MeV [6–9].

Recent light-emulsion CNO nuclei experiments at KEK [11] and J-PARC [12] may bring a glimmer of enlightenment to this discrepancy, as they provide a complete identification of the final decay products after the  $\Xi^-$  capture. Particularly interesting are the events in which a pair of single- $\Lambda$  hypernuclei are produced in the final state, namely  $\Xi^- + {}^A Z \rightarrow {}_{\Lambda}^{A'} Z' + {}_{\Lambda}^{A''} Z''$ . This is because the two  $\Lambda$  particles must be in a  $1s_{\Lambda}^2$  state, so that in the capture process,  $\Xi^- p \rightarrow \Lambda\Lambda$ , the  $\Xi^-$  must satisfy  $l_{\Xi^-} = l_p$ . Since the  $^{12}\text{C}$ ,  $^{14}\text{N}$  and  $^{16}\text{O}$  components of the emulsion are all p-shell nuclear targets, the choice  $l_{\Xi^-} = 1$  is favored in these events.

In Table I we show the binding energies  $B_{\Xi^-}$  reported by the two experiments. We note that the values are about 1 MeV, significantly higher than the purely-Coulomb atomic 2P binding energies. A recent theoretic-

Experiment	${}^A Z \quad {}_{\Lambda}^{A'} Z' + {}_{\Lambda}^{A''} Z''$	$B_{\Xi^-}$ (MeV)
KEK E176 [11]	${}^{12}\text{C} \quad {}_{\Lambda}^4\text{H} + {}_{\Lambda}^9\text{Be}$	$0.82 \pm 0.17$
J-PARC E07 [12]	${}^{14}\text{N} \quad {}_{\Lambda}^5\text{He} + {}_{\Lambda}^{10}\text{Be}$	$1.27 \pm 0.21$

TABLE I: Reported two-body  $\Xi^-$  capture events  $\Xi^- + {}^A Z \rightarrow {}_{\Lambda}^{A'} Z' + {}_{\Lambda}^{A''} Z''$  in light-emulsion nuclei to a pair of single- $\Lambda$  hypernuclei.

cal analysis of these pair of  $\Lambda$ -hypernuclei events has been done [10], reaching the conclusion that the  $\Xi^-$ -nucleus well potential depth is of  $V_{\Xi} \approx 24$  MeV. The strength of this  $\Xi^-$ -nuclear potential is determined by requiring that it reproduces the  $1p_{\Xi^-}$  nuclear state in  $^{12}\text{C}$  bound by  $0.82 \pm 0.17$  MeV.

The former study is the backbone of this paper. Indeed, in the present work we aim at carrying out a similar analysis on the basis of a simpler potential model. Our desire is to find how  $\Xi^-$  *atomic* and *nuclear* bound states depend on the nuclear potential well depth and to develop a program capable of finding accurately the  $\Xi^-$ -nuclear energy levels, which is easy to adapt to other potential functions, interacting particles or nuclei.

## II. FORMALISM

### A. Schrödinger's equation

Our goal is to resolve the  $\Xi^-$ -nucleus system, finding the energy levels and their dependence on the nuclear well depth potential. We have considered  $M_{\Xi^-} = 1321.31$  MeV/ $c^2$  and  $M_N = A \cdot M_p$  where  $M_p = 938.27$  MeV/ $c^2$  is the proton mass and  $A$  is the mass number. The model used is based on solving the radial Schrödinger's equation:

$$\frac{d^2 P_{nl}(r)}{dr^2} + \left( \frac{2\mu}{\hbar^2} (E - V(r)) - \frac{l(l+1)}{r^2} \right) P_{nl}(r) = 0 \quad (1)$$

$$P_{nl}(r) = rR_{nl}(r) \quad , \quad (2)$$

where  $P_{nl}(r)$  is the reduced radial function,  $\mu$  is the reduced mass of the two-body system and  $\hbar$  is the reduced Planck constant.

## B. Potentials

The potential  $V(r)$  will be the sum of a Coulomb potential  $V_c(r)$  -to which we have implemented the nucleus finite-size corrections- and a nuclear potential  $V_{WS}(r)$  modelled as a Woods-Saxon function:

$$V_c(r) = \begin{cases} -\frac{Ze^2}{R_N} \left( \frac{3}{2} - \frac{r^2}{2R_N^2} \right) & \text{if } r \leq R_N \\ -\frac{Ze^2}{r} & \text{if } r > R_N \end{cases} \quad (3)$$

$$V_{WS}(r) = -\frac{V_0}{1 + e^{\frac{r-R_N}{a}}} \quad , \quad (4)$$

where  $a = 0.5$  fm is the surface thickness of the nucleus,  $V_0$  is the potential well depth and  $R_N = r_0(A)A^{1/3}$  is the nucleus radius. The function  $r_0(A)$  is taken from the parametrization of Ref. [19]:

$$r_0(A) = 1.128 + 0.439A^{-2/3} \quad (5)$$

The former potentials are depicted in Fig.1.

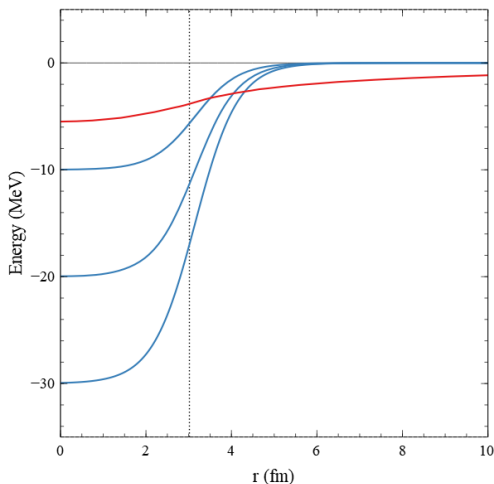


FIG. 1: Finite-size Coulomb potential (red line) and nuclear Woods-Saxon potential (blue lines) with  $V_0 = 10, 20, 30$  MeV for  $^{16}\text{O}$ . The radius of the nucleus,  $R_N = 3.016$  fm, is marked by a vertical dotted line.

## C. Numerical solution

Equation (1) is a second order differential equation which has no analytical solution, *i.e.* should be solved

numerically. We have utilized Numerov's algorithm [17], which resolves generic second order differential equations of the type:

$$\frac{d^2u(r)}{dr^2} = -g(r)u(r) + s(r) \quad (6)$$

Comparing (1) and (6), one can easily identify:

$$g(r) = \left( \frac{2\mu}{\hbar^2}(E - V(r)) - \frac{l(l+1)}{r^2} \right)$$

$$s(r) = 0 \quad u(r) = P_{nl}(r)$$

The Numerov's method consists of discretizing equation (6), where the solution  $u(r)$  is expanded up to the fourth order. The resulting Numerov's formula is:

$$u_{n+1} = \frac{(12 - 10f_n)u_n - f_{n-1}u_{n-1}}{f_{n+1}} \quad (7)$$

where:

$$f_n \equiv 1 + g_n \frac{(\Delta r)^2}{12} \quad (8)$$

and  $\Delta r$  is the discretization step.

## D. Methodology

### 1. Atomic states

Solving Schrödinger's equation (1) is an eigenvalue problem. The idea here is to numerically integrate (1) forward -from  $r = 0$  to  $r = r_{match}$ - and backwards -from infinity to  $r = r_{match}$ - and request to the solutions  $u(r)$  to fulfill some continuity conditions at  $r_{match}$ .

For bound atomic levels, the matching point  $r_{match}$  is chosen to be the classical turning point of the particle, *i.e.* where the energy of the particle equals the potential energy:

$$r_t = \frac{a\mu}{Z} \left[ n^2 + \sqrt{n^4 - n^2l(l+1)} \right] \quad (9)$$

In order to use Numerov's method we have to give the first two points -or the last two in backwards integration- of the mesh. So, we must set the boundary conditions:  $u(0) = 0$  and  $u(\infty) = 0$ . Moreover, by analogy to the wave functions of the hydrogen atoms, we should expect the following behaviours:

$$u(r) \xrightarrow{r \rightarrow 0} r^{l+1} \quad (10)$$

$$u(r) \xrightarrow{r \rightarrow \infty} \exp(-Zr/na_\mu) \quad (11)$$

We defined the "numerical" infinity as  $200R_N$ .

### 2. Nuclear states

In the case of nuclear states, the wave function is much closer to nucleus. The matching point is set to be the nuclear radius  $R_N$ , given by Eq. (5). The behaviour in the boundaries is consider to be [13]:

$$u(r) \xrightarrow[r \rightarrow 0]{} r^{l+1} \quad (12)$$

$$u(r) \xrightarrow[r \rightarrow \infty]{} \exp(-r/R_N) \quad (13)$$

We defined the “numerically” infinity as  $30R_N$ .

### 3. Bisection method and continuity requests

For the purpose of finding the eigenvalues  $E$  and eigenfunctions  $P_{nl}(r)$  that resolve Eq. (1), we use the bisection method, which, though primitive, is a powerful technique. So, we feed our program with two energies and it will numerically integrate forward and backwards to the matching point for both energies. We must impose to our solutions an smooth continuity in  $r_t$ , *i.e* they must satisfy:

$$\frac{1}{u_m^{(F)}} \frac{du^{(F)}}{dx} \Big|_{r_{match}} - \frac{1}{\tilde{u}_m^{(B)}} \frac{d\tilde{u}^{(B)}}{dx} \Big|_{r_{match}} = 0 \quad (14)$$

Where  $u^{(F)}$  and  $\tilde{u}^{(B)}$  stands for the forward and backward integration, respectively; and  $u_m = u(r_{match})$ .

If the wave functions found do not sort out (14) for any value of the two chosen energies, the bisection algorithm will change these values, calculating their eigenfunctions by Numerov’s, until it finds an energy linked to a wave function that correctly accomplish the continuity request. That will correspond to an energy level of the  $\Xi^-$  atom. It must be clarified that the wave function found is not yet the correct one, as it has to be modified by an overall factor  $\alpha = u_m^{(F)} / \tilde{u}_m^{(B)}$ :

$$u^{(B)}(r) = \alpha \tilde{u}^{(B)}(r) \quad (15)$$

In Fig. 2 the lowest  $\Xi^-$  states for a nuclear potential well depth of  $V_0 = 10$  MeV in  $^{12}\text{C}$  are shown.

## III. RESULTS

We have focused our studies on the interaction of  $\Xi^-$  with  $^{12}\text{C}$ ,  $^{14}\text{N}$  and  $^{16}\text{O}$ . The program developed is able to find the ground and excited states for a specific  $L$  value. As we are currently interested in the lowest atomic states, Table II shows the lowest  $\Xi^-$  energy levels of  $L = 0$  and  $L = 1$  in different atoms. The greater the potential well depth  $V_0$  is, the more attractive the energy levels become. Obviously, this effect is more pronounced in the lowest

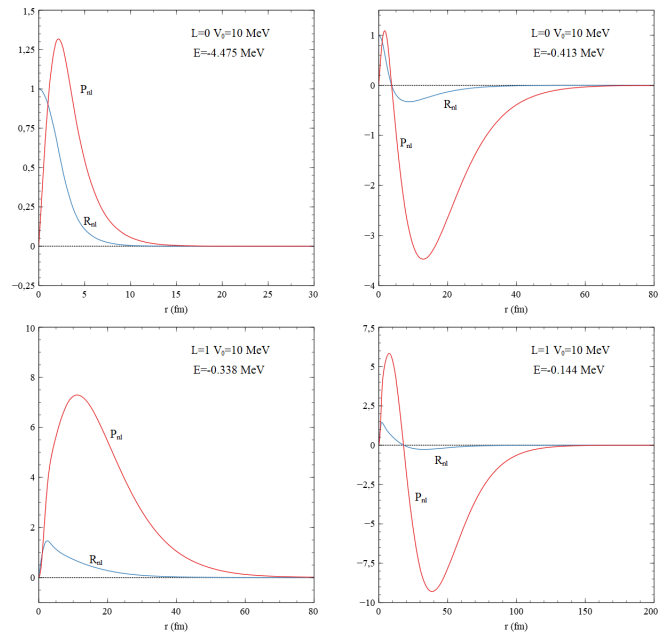


FIG. 2: From left to right, up to down: wave functions of the lowest  $\Xi^-$  states (1S, 2S, 2P, 3P) in  $^{12}\text{C}$  for a nuclear potential depth  $V_0 = 10$  MeV. Radial functions  $R_{nl}(r)$  are shown in blue and reduced radial functions  $P_{nl}(r)$  in red.

(MeV)		Coulomb	$V_0 = 10\text{MeV}$	$V_0 = 20\text{MeV}$	$V_0 = 30\text{MeV}$
$^{12}\text{C}$	(1S)	-0.950	-4.475	-10.920	-18.414
	(2S)	-0.259	-0.413	-0.507	-0.734
	(2P)	-0.283	-0.338	-2.059	-6.789
	(3P)	-0.126	-0.144	-0.238	-0.2659
$^{14}\text{N}$	(1S)	-1.243	-5.330	-12.157	-19.924
	(2S)	-0.392	-0.539	-0.679	-1.163
	(2P)	-0.391	-0.567	-3.265	-8.618
	(3P)	-0.174	-0.224	-0.326	-0.353
$^{16}\text{O}$	(1S)	-1.554	-6.128	-13.263	-21.250
	(2S)	-0.477	-0.676	-0.884	-1.772
	(2P)	-0.515	-0.929	-4.437	-10.270
	(3P)	-0.229	-0.321	-0.424	-0.460

TABLE II: Energy levels (in MeV) of the lowest  $\Xi^-$  atomic levels in  $^{12}\text{C}$ ,  $^{14}\text{N}$  and  $^{16}\text{O}$ , modelled by different well potentials depths.

energy levels (1S, 2P). Furthermore, the more nucleons the atom has, the deeper will the energies be.

Fig. 3, Fig. 4 and Fig. 5 present the evolution of the lowest portion of the nuclear/atomic spectrum of  $\Xi^-$  in  $^{12}\text{C}$ ,  $^{14}\text{N}$  and  $^{16}\text{O}$ , where all behave the same way. Energy levels start at  $V_0 = 0$  MeV as purely atomic 1S, 2P, 2S, 3P states from bottom up. With the increase of the nuclear potential well depth, the 1S state dives down in energy quickly, overlapping with the nuclear core and becoming indistinguishable from a nuclear 1s state. The

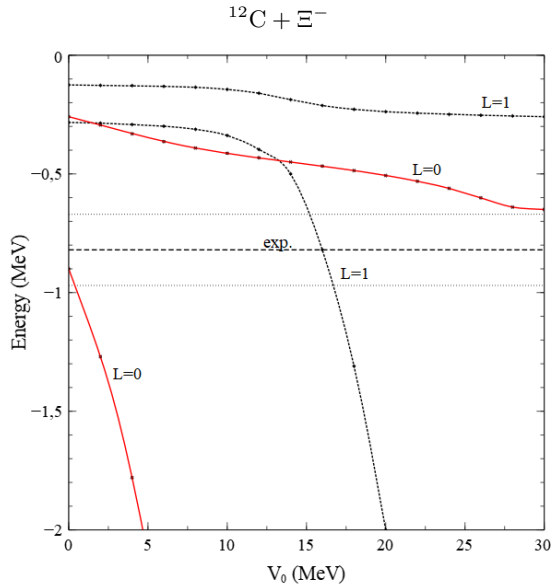


FIG. 3: Lowest  $\Xi^-$  energy levels (in MeV) for  $L = 0$  (1S,2S) and  $L = 1$  (2P,3P) in  $^{12}\text{C}$  as a function of  $V_0$ . The dashed and dotted horizontal lines indicate the binding energy  $B_{\Xi^-} = -0.82 \pm 0.15$  MeV from TABLE I

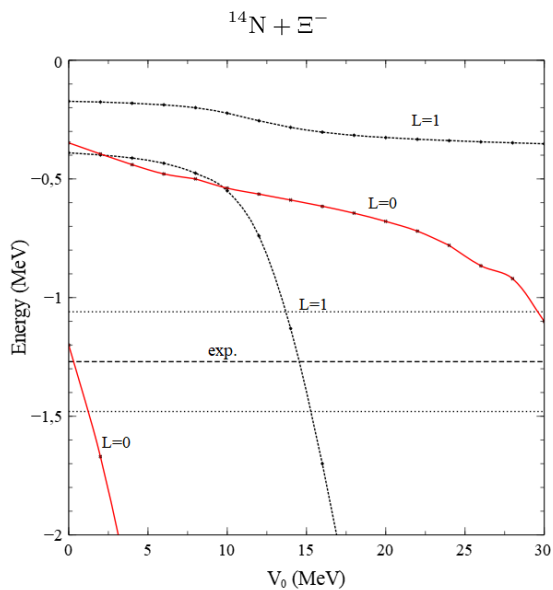


FIG. 4: Lowest  $\Xi^-$  energy levels (in MeV) for  $L = 0$  (1S,2S) and  $L = 1$  (2P,3P) in  $^{14}\text{N}$  as a function of  $V_0$ . The dashed and dotted horizontal lines indicate the binding energy  $B_{\Xi^-} = -1.27 \pm 0.21$  MeV from TABLE I.

next atomic state to decline sharply to the nuclear spectrum is 2P, for  $V_0 \gtrsim 15$  MeV in  $^{12}\text{C}$ ,  $V_0 \gtrsim 10$  MeV in  $^{14}\text{N}$  and  $V_0 \gtrsim 7.5$  MeV in  $^{16}\text{O}$ . While the 2P atomic state becomes the nuclear 1p state, the 2S and 3P ones slowly decrease their energies in order to rearrange the spectrum, becoming the 1S and 2P atomic states, respec-

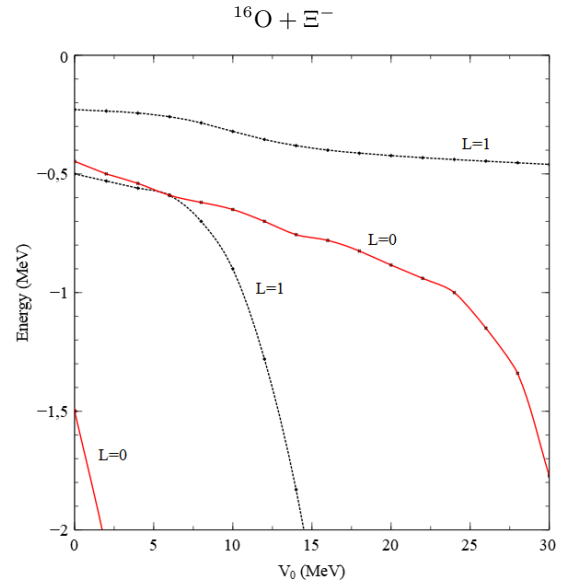


FIG. 5: Lowest  $\Xi^-$  energy levels (in MeV) for  $L = 0$  (1S,2S) and  $L = 1$  (2P,3P) in  $^{16}\text{O}$  as a function of  $V_0$ .

tively [14].

Considering the experimental values of the binding energies and their errors, marked by straight lines in Fig. 3 and Fig. 4, we propose that both events -KEK E176 and J-PARC E07- listed in Table I are compatible with a  $1p_{\Xi^-}$  nuclear state -evolved from an atomic 2P one- related to a nuclear potential depth of  $V_0 \sim 14 - 17$  MeV. This result differs from the  $\Xi^-$ -nuclear potential of  $V_{\Xi^-} \approx 24$  MeV conclude in [10].

On our purpose to understand the mismatch between the potential well depth our outcomes suggest and the one conclude in [10], we have studied how some parameters, as the surface thickness  $a$  and the nucleus radius  $R_N$ , from the nuclear potential used (4), affect the results we obtain. Also, one may think that this discrepancy may be caused by using different nuclear potential expressions. In [10] an optical potential is applied and spin and isospin degrees of freedom are taken in account. However, the imaginary part is too small to make both results differ that much, as it contributes just as the 3% of the full optical potential.

#### IV. CONCLUSION

We have shown how sensitive the  $\Xi^-$  nuclear bound states are to the potential well depth  $V_0$  of a Woods-Saxon shaped potential (4) and how, while it increases, the original atomic 1S and 2P states evolve to 1s and 1p nuclear states, hence rearranging the energy spectrum. Furthermore, the code programmed has allowed us to resolve the Schrödinger's equation (1) effectively and to obtain the precisely energy levels of  $\Xi^-$  atom for a given  $V_0$ .

We have demonstrated that both two-body  $\Xi^-$  capture events in light-emulsion nuclei reported in KEK [11] and J-PARC [12], producing a pair of single- $\Lambda$  hypernuclei from Table I, matches with a  $1p_{\Xi^-}$  nuclear state with a  $\Xi^-$ -nuclear potential depth of  $V_0 \sim 14 - 17$  MeV. Earlier predicted by [10], their work reaches a quite different value of  $V_{\Xi} \approx 24$  MeV and some considerations has been taken in account in order to justify the gap between both studies. Unfortunately, no overall definitive conclusion about this discrepancy has been drawn.

We have successfully compared the energy levels obtained from our program with the ones displayed on different works as [15], [20] and [21]. So, it is fair to say that a simple and easy to adapt method has been developed. Our algorithm could be useful in future trials with new results as J-PARC E05 and E70 ( $K^-, K^+$ ) experiments on  $^{12}\text{C}$ [18].

Studying  $\Xi^-$ -nuclear interaction is vital to gain knowledge about how strangeness  $S = -2$  hyperons relate with

nuclear media. Understanding how they interact with the environment they are embedded, *e.g.* light-emulsions experiments like the ones commented in the introduction [11, 12], could allow us improve in solving the Hyperon Puzzle, which addresses the fate of hyperons in dense neutron-star matter [16], and in advancing in knowledge of strange hadronic matter and they role in the universe.

### Acknowledgments

I would like to express my gratitude to my advisor, Dra. Àngels Ramos, for his guidance and help in the development of this work. I would also like to thank my friends for always being by my side and to my family, especially to my father, for their support and their trust on me.

- 
- [1] S. Acharya, et al., ALICE Collaboration, Phys. Rev. C 99 (2019) 024001.
  - [2] S. Acharya, et al., ALICE Collaboration, Phys. Lett. B 797 (2019) 134822.
  - [3] S. Acharya, et al., ALICE Collaboration, Phys. Rev. Lett. 123 (2019) 112002.
  - [4] S. Acharya, et al., ALICE Collaboration, Nature 588 (2020) 232.
  - [5] C.B. Dover and A. Gal, Ann. Phys. (N.Y.)146, 309 (1983).
  - [6] T. Fukuda, et al., E224 Collaboration, Phys. Rev. C 58 (1998) 1306.
  - [7] P. Khaustov, et al., The AGS E885 Collaboration, Phys. Rev. C 61 (2000) 054603.
  - [8] J.K. Ahn, et al., Phys. Rev. Lett. 87 (2001) 132504.
  - [9] T. Harada, Y. Hirabayashi, Phys. Rev. C 103 (2021) 024605.
  - [10] Friedman, E, and A Gal. "Constraints on  $\Xi^-$  Nuclear Interactions from Capture Events in Emulsion." Physics letters. B 820 (2021): 136555-. Web.
  - [11] S. Aoki, et al., KEK E176 Collaboration, Nucl. Phys. A 828 (2009) 191.
  - [12] S.H. Hayakawa, et al., J-PARC E07 Collaboration, Phys. Rev. Lett. 126 (2021) 062501.
  - [13] López de Arbina de Frutos, I. (2018). Nuclear quasi-bound states of antikaons and  $\eta$  mesons. (Trabajo Fin de Máster Inédito). Universidad de Sevilla, Sevilla.
  - [14] A. Gal, E. Friedman, C.J. Batty, Nucl. Phys. A 606 (1996) 283.
  - [15] C.J. Batty, E. Friedman, A. Gal, Phys. Rev. C 59 (1999) 295.
  - [16] L. Tolos, L. Fabbietti, Prog. Part. Nucl. Phys. 112 (2020) 103770.
  - [17] B. V. Numerov, Mon. Not. Roy. Astron. Soc., 84 592.
  - [18] T. Nagae, et al., AIP Conf. Proc. 2130 (2019) 020015.
  - [19] D. J. Millener, C. B. Dover, and A. Gal Phys. Rev. C 38, 2700
  - [20] A. Baca, C. García-Recio, J. Nieves, Nucl. Phys. A 673 (2000) 335353
  - [21] Gamarra Arbina, M. (2020)"An analysis of the nuclear interaction with  $\Xi^-$  atoms".(Treball Fi de Grau). Universitat de Barcelona, Barcelona.